

Enhanced dechlorination of tetrachloroethylene by polyethylene glycol-coated zerovalent silicon in the presence of nickel ions

Chun-chi Lee, Ruey-an Doong*

Department of Biomedical Engineering and Environmental Sciences, National Tsing Hua University, 101, Sec. 2, Kuang Fu Road, Hsinchu, 30013, Taiwan

ARTICLE INFO

Article history:

Received 8 March 2013

Received in revised form 27 May 2013

Accepted 28 June 2013

Available online 8 July 2013

Keywords:

Polyethylene glycol (PEG)

Tetrachloroethylene (PCE)

Nickel ions

Synergistic effect

Hydrodechlorination

ABSTRACT

In this study, the combined effect of polyethylene glycol (PEG) and nickel ions on the dechlorination of tetrachloroethylene (PCE) by zerovalent silicon (Si(0)) under anoxic conditions was investigated. PEG was first coated onto the surface of Si(0) to form PEG-coated Si(0) (Si_{PEG}) and the concentration effect of Ni(II) ions at 0.001–2 mM on the dechlorination of PCE by Si_{PEG} was evaluated and optimized. Results of X-ray photoelectron spectroscopy and electron probe microanalysis showed that addition of PEG can not only inhibit the formation of SiO_2 but also change the distribution pattern of SiO_2 from homogeneous distribution to discrete and localized dispersion, resulting in the enhancement of dechlorination efficiency and rate of PCE by Si(0). The dechlorination of PCE by Si_{PEG} followed pseudo-first-order kinetics and the pseudo-first-order rate constant (k_{obs}) for PCE dechlorination was $0.36 \pm 0.02 \text{ h}^{-1}$. Addition of Ni(II) exhibited the synergistic effect on the enhanced dechlorination of PCE by Si_{PEG} , and the maximum k_{obs} for PCE dechlorination was $0.79 \pm 0.02 \text{ h}^{-1}$, which corresponded to 220–335 times higher than that by Si(0) alone. Hydrogenolysis and hydrodechlorination occurred simultaneously for PCE dechlorination by bimetallic Ni/ Si_{PEG} system in the presence of Ni(II) ions, and the product distribution was highly dependent on the mass loading of Ni ions. The surface coverage of Ni onto Si_{PEG} was used to well describe the synergistic effect of Ni(II) and Si_{PEG} on the enhanced dechlorination of PCE by Si(0) under anoxic conditions.

© 2013 Elsevier B.V. All rights reserved.

1. Introduction

Zerovalent iron (ZVI) has been widely used as a reductive material for the dechlorination of chlorinated hydrocarbons such as tetrachloroethylene (PCE) and trichloroethylene (TCE) in aquatic environments [1–3]. The dechlorination of PCE and TCE by ZVI is a surface-mediated reaction and is largely controlled by the available surface sites [4–6]. However, the formation of iron oxides on the surface of ZVI decreases the dechlorination efficiency and rate of chlorinated hydrocarbons [7]. In addition, the use of sodium borohydride as the reducing agent to produce nanoscale ZVI may generate and release boron/boron oxide nanoparticles, which can deposit on environmental media and be toxic to organisms [8,9]. Recently, zerovalent silicon (Si(0)) has been demonstrated as a promising material for dechlorination of PCE and carbon tetrachloride [10–12]. Silicon is the second most abundant element in the earth's crust and the cost-benefit is comparable to that of ZVI. A previous study has shown that the reaction rate of PCE dechlorination by Si(0) was 1.5–2.4 times higher than that by ZVI [12]. However, TCE was the major product for PCE dechlorination by Si(0). The

addition of second catalytic metal ions can increase the dechlorination rate as well as change the distribution of end products [13–16]. Lee and Doong [11] have recently reported that the reaction mechanism for PCE dechlorination changed from reductive dechlorination to hydrodechlorination in the presence of bimetallic Ni/Si. In addition, the dechlorination rate of PCE by bimetallic Ni/Si increased 15 times when compared with Si(0) alone, clearly showing the superior reactivity of Ni/Si toward PCE dechlorination.

In addition to the second catalytic metal ions, the increase in electron transfer from the reductive metal to chlorinated hydrocarbons in the presence of electron mediators such as surfactants and humic acid is another strategy for the enhancement of dechlorination efficiency [17,18]. Cetyltrimethylammonium bromide (CTAB), sodium dodecyl sulfate, and Tween 80 are commonly used surfactant in ZVI system [19–21]. Alessi and Li [21] reported that the rate constant for PCE dechlorination increased by factors of 4–19 after adding CTAB to the ZVI system. Our previous study has indicated that polyethylene glycol (PEG) and CTAB could significantly increase the dechlorination efficiency and rate of PCE removal by Si(0) and the reaction rate enhanced by PEG was 1.7 times higher than that by CTAB [10]. Different from the enhanced solubilization of PCE by CTAB, addition of PEG can prevent the formation of silicon dioxide (SiO_2) on Si(0) surface, and further enhances the reaction rate of PCE dechlorination by a factor of

* Corresponding author. Tel.: +886 3 5726785; fax: +886 3 5718649.

E-mail address: radoong@mx.nthu.edu.tw (R.-a. Doong).

106 at pH 8.3 ± 0.2 . However, the reaction mechanism for PCE dechlorination by Si(0) in the presence of PEG remains unclear.

PEG is a bi-functional amphiphilic polymer with reactive hydroxyl groups on both ends with the advantages of high water solubility, non-toxicity, low cost, and environmental friendliness. Our previous study has indicated that the surface modification with PEG is a simple method to enhance the reactivity of Si(0) toward chlorinated compound dechlorination [10]. In addition, PEG can serve as a cross-linker to immobilize the nanoscale zerovalent metals onto the support and as a chelating agent for adsorption of metal ions [22,23]. Similar to the ZVI, Si(0) is a strong reducing material which can reduce the catalytic metal ions such as Ni²⁺ and Cu²⁺ into the reduced species to form bimetallic Cu/Si and Ni/Si systems for the increase in dechlorination rate of chlorinated hydrocarbon [11,24]. This gives a great impetus to understand the combined effect of nickel ions and PEG on the enhanced dechlorination of PCE by Si(0). However, the synergistic effect of nickel ions and PEG on the dechlorination of PCE by Si(0) has been rarely reported.

In this study, the synergistic effect of nickel ions and PEG on the dechlorination efficiency and rate of PCE by Si(0) was investigated under anoxic conditions. PEG was first coated onto the surface of Si(0) to form PEG-coated Si(0) (Si_{PEG}) and the concentration effect of Ni(II) ions on the dechlorination of PCE by Si_{PEG} was evaluated and optimized. X-ray photoelectron spectroscopy (XPS), scanning electron microscopy (SEM) and electron probe microanalysis (EPMA) were utilized to characterize the change in morphology and metal species on the surface of Si(0) before and after the addition of PEG and nickel ions. In addition, the product distribution as well as reaction mechanism for PCE dechlorination by Si_{PEG} in the presence of various mass loadings of Ni(II) was determined.

2. Materials and methods

2.1. Chemicals

Tetrachloroethylene (PCE) (>99.8%, GC grade), trichloroethylene (TCE) (>99.8%, GC grade), and PEG (MW 2000–35,000) were purchased from Sigma-Aldrich Co. (Milwaukee, WI). Tris(hydroxymethyl) aminomethane (Tris buffer) (reagent grade), and zerovalent silicon (>99.5% purity, <100 µm) were purchased from Merck Co. (Darmstadt, Germany). All other chemicals were of analytical grade and were used as received without further purification. Solutions were prepared with high-purity deoxygenated deionized water (Millipore, 18.3 MΩ cm) using a vacuum and N₂ (>99.99%) purging system.

2.2. Preparation of PEG pre-coated silicon (Si_{PEG})

The PEG pre-coated Si(0) was prepared according to our previous work with minor modification [10]. Briefly, 0.5 g of HF-washed Si(0) and 17.5 µg of PEG with various molecular weights ranging from 2000 to 35,000 was added into a 60-mL serum bottle for preparation of Si_{PEG}. After adding 25 mL of anoxic bidistilled deionized water (DI H₂O) and equilibration for 3 h under stirring, the Si_{PEG} was harvested by centrifugation at 6944×g for 5 min and dried by a gentle flow of N₂ gas. Fig. S1 shows the SEM images of HF-washed and PEG-coated Si(0). A smooth surface of fresh Si(0) was observed after washing with HF. However, some white spots were observed onto the surface of Si_{PEG}, presumably attributed to the formation of SiO₂ during the coating of PEG onto Si(0). The XPS spectrum of Si_{PEG} (Fig. S2) showed peaks at 99.4 and 104 eV, which can be assigned as Si(0) and SiO₂, respectively. This means that parts of the silicon surface were oxidized to silica during the preparation step of Si_{PEG}. In addition, the molecular weight as well as carbon length of PEG

has little influence on the enhancement of dechlorination efficiency and rate of PCE when the added amounts of PEG are the same (Fig. S3). Therefore, PEG-35000 was selected as the model compound for further experiments.

2.3. Dechlorination experiments.

Experiments were conducted in batch-fed modes using serum bottles sealed with Teflon-lined rubber septa and aluminum crimp caps. In addition, all the serum bottles were initially stored in the anaerobic glove box to maintain the anoxic conditions. 60 mL serum bottles were filled with 0.05 g Si_{PEG}. After being capped with Teflon-lined rubber septa with aluminum crimp caps (The Wheaton Co., NJ), the sealed serum bottles could maintain the anaerobic conditions. Since all the anoxic solutions were prepared using vacuum and N₂-pruning system outside the glove box, serum bottles were transported outside the glove box, and then filled with 25 mL of deoxygenated buffer solutions by 25 mL N₂-purged syringe under anoxic conditions. 50 mM Tris buffer solution was used to control the pH at 8.3 ± 0.1 . The stock solution of PCE dissolved in deoxygenated methanol was introduced into the Si_{PEG} system to get a final concentration of 60 µM. In addition, stock solutions of Ni(II) were added into the serum bottles to obtain the final concentrations of 0.001–2 mM. The total volume of the liquid phase was 25 mL, resulting in a 35-mL headspace left for headspace analysis. The bottles were incubated with an orbital shaker at 120 rpm and at $25 \pm 1^\circ\text{C}$ in the dark to well-suspend the Si_{PEG} and bimetallic Ni-Si_{PEG} particles and to minimize the mass transfer limitation in the batch experiments [10–12]. The XPS spectrum of bimetallic Ni/Si_{PEG} particles shown in Fig. S4 clearly indicated two peaks located at 852.7 and 869.9 eV, which corresponded to 2p_{2/3} and 2p_{1/2} of Ni(0). Parallel experiments were also carried out without the addition of zerovalent silicon. All the experiments were run in duplicate or triplicate.

It is known that the dechlorination of chlorinated hydrocarbons by zerovalent metals is a surface-mediated reaction, and Langmuir-Hinshelwood kinetic model can be used to elucidate the reaction kinetics on the Si_{PEG} surface:

$$r = \frac{dC}{dt} = k_{app} \frac{K_L S_t C}{1 + K_L C} \quad (1)$$

where C is the aqueous concentration of PCE, k_{app} is the limiting-step rate constant of reaction at maximum coverage under the given conditions, S_t is the abundance of reactive sites, and K_L is the Langmuir adsorption coefficient of PCE on reactive sites. Zhu et al. [18] used Langmuir–Hinshelwood kinetic model to elucidate the reaction kinetics of trichlorobenzene on the amphiphile-modified Pd/Fe surface, and found a reasonable consistency between the changes of the pseudo-first-order rate constants (k_{obs}) and $k_L S_t$ with changing amphiphile concentrations. When the concentration C is low and $K_L C \ll 1$, Eq (1) can be simplified to the pseudo-first-order kinetics.

2.4. Analytical methods

The headspace analytical technique was used for the determination of chlorinated hydrocarbons and non-chlorinated hydrocarbons. The concentrations of PCE and the byproducts in the headspace of the test bottles were monitored by withdrawing 40 µL of gas in the headspace using a 50-µL gas-tight syringe. The headspace sample was immediately injected into a gas chromatograph (GC) equipped with an electron capture detector (ECD) and a flame ionization detector (FID) (PerkinElmer, Autosystem, Norwalk, CT). A 60-m VOCOL fused-silica megabore capillary column (0.545 mm × 3.0 µm, Supelco Co.) was used to separate the organic compounds. The column was connected to the FID

and ECD simultaneously by a Y-splitter; and an optimal sensitivity for chlorinated hydrocarbons was achieved with 40% of the flow (1.85 mL min^{-1}) to ECD. The column temperature was isothermally maintained at 120°C using ultra-high purity nitrogen (>99.9995%) as the carrier gas. The temperatures of the ECD and FID were maintained at 325 and 220°C , respectively. ECD was used to quantify the change in concentrations of PCE and TCE, while FID was employed to determine *cis*-DCE, VC and ethane. In addition, an Agilent 6890 GC connected with an Agilent 5973 mass selective detector was used to identify the products of PCE dechlorination, and found that concentrations of *trans*-DCE, 1,1-DCE, acetylene and ethylene were below the detection limits. The relative standard deviations (RSDs) of the ECD analyses were within 10% and those for the FID analyses were within 5%. Control samples were also used to check the possible leakage of target compounds during the incubation process. In addition, the calibration curves of chlorinated hydrocarbons were prepared using the external standard method by preparing the known concentrations of chlorinated hydrocarbons in aqueous solutions at 25°C . Aqueous concentrations of chlorinated hydrocarbons in tested bottles were calculated using the calibration curves obtained from the external standard method.

The volume of gas produced from the reaction of Si(0) with water was measured by inserting a 20-mL glass syringe into the serum bottles. The XPS measurements were performed by an ESCA PHI 1600 photoelectron spectrometer (Physical Electronics, Eden Prairie, MN) using Al K α X-ray source ($1486.6 \pm 0.2 \text{ eV}$ photon energy). The spherical capacitor analyzer with a multi-channel detector had a takeoff angle of 70° related to the horizontal of the sample plane. The data were recorded digitally, and all peak scans were signal averaged until an acceptable signal-to-noise ratio was obtained. During the data acquisition, the pressure in the sample chamber did not exceed 2.5×10^{-8} Torr. The binding energies of the photoelectrons were determined under the assumption that carbon has a binding energy of 284.8 eV .

EPMA was performed using an electron probe X-ray microanalyzer (JEOL JXA-8200) with an accelerating voltage of 20 kV and a beam current of 20 nA . The K α line of Ni was measured on four wavelength-dispersive spectrometers to minimize beam damage to the sample. Nickel metal was used as the standard for Ni determination. In addition, the surface morphology of the Si_{PEG} and Ni-Si_{PEG} was determined by SEM (JEOL JSM-6700F Oxford Inca Energy 400) equipped with a back scattering detector. All the samples were Au-coated using Ion Sputter s-1030 (Hitachi, Japan). The accelerating voltage and the applied current were 10 kV and 20 nA , respectively. After coating with Au, samples were placed under high vacuum (10^{-3} to 10^{-7} mbar) conditions. The scanning electron image (SEI) resolution was 1.5 nm at 15 kV and 5 nm at 1.0 kV .

3. Results and discussion

3.1. Surface characterization of Si_{PEG}

To elucidate the effect of PEG on the reactivity of Si(0), the change in distribution patterns of silicon species on fresh Si(0) and Si_{PEG} was characterized by XPS. Fig. 1 shows the XPS spectra of Si species on the surface of fresh Si(0) and Si_{PEG} particles at various reaction times. The XPS spectra of fresh Si(0) in the absence of PEG showed a peak at 99.5 eV , which is a characteristic peak of unreacted bulk silicon (Si $2p_{3/2}$). Another peak at 103 – 105 eV which is attributed to SiO₂ and SiO groups appeared in XPS spectra after 3 h of incubation, and the peak intensity increased from 3 to 24 h , indicating the increase in generated SiO₂ on the surface of Si(0). Different from the fresh Si(0), the XPS spectra of Si_{PEG} showed two peaks centered at 99.5 and 103 – 105 eV initially and the peak intensity only changed slightly with time, indicating the stability of

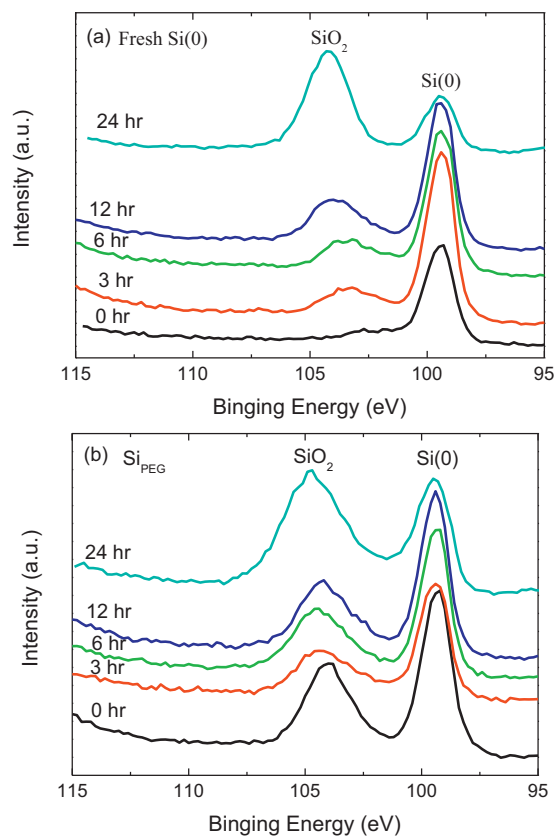


Fig. 1. The XPS spectra of Si species on the surface of (a) fresh Si(0) and (b) Si_{PEG} particles at various reaction times.

Si(0) surface after coating with PEG. Table S1 shows the change in formation ratios of SiO₂ on the surfaces of Si_{PEG} and fresh Si(0). The silicon dioxide was generated rapidly on the fresh Si(0) surface in the absence of PEG, and the ratio increased from 27% at 3 h to 73% at 24 h . In contrast, the formation ratio of SiO₂ on Si_{PEG} maintained stably at 47–48% in the first 12 h and then slightly increased to 57% after incubation of 24 h , showing that addition of PEG can maintain the reactivity of Si(0). It is noteworthy that the initial ratio of SiO₂ on Si_{PEG} was 47%, which was higher than that of fresh Si(0). This is mainly attributed to the time needed for preparation of Si_{PEG}. For preparation of Si_{PEG}, PEG was equilibrated with fresh Si(0) for 3 h in solution and then underwent the centrifugation and drying, resulting in the formation of SiO₂ onto the Si_{PEG} during the preparation processes. Once PEG was coated onto the surface of Si(0), however, the reactivity of Si(0) toward PCE dechlorination was maintained.

EPMA was further used to characterize the distribution patterns of SiO₂ on the surface of Si(0) and Si_{PEG} after the reaction with buffer solution for 6 h . Since both Si(0) and SiO₂ contain Si element, O element was then used for EPMA mapping to elucidate the difference in distribution patterns of SiO₂ between fresh Si(0) and Si_{PEG}. As shown in Fig. 2, the discrete and localized distribution of SiO₂ on the Si_{PEG} surface was clearly observed after 6 h of incubation, presumably attributed to the bridging function of PEG on SiO₂. Zhang et al. depicted that PEG is a bi-functional chemical which could cause the phase separation by bridging flocculation, and resulted in the good dispersivity of SiO₂ spheres [25,26]. In addition, divalent ions play a crucial role between polymer-particle interactions, and the enhancement of Si(0) nanoparticle aggregation in the presence of Suwannee River humic acid was found to be attributed to the bridge formation in the Ca $^{2+}$ solutions [27]. On the contrary, the distribution pattern of oxygen element on Si(0) surface in the absence of PEG was homogeneous and the intensity was higher than that of

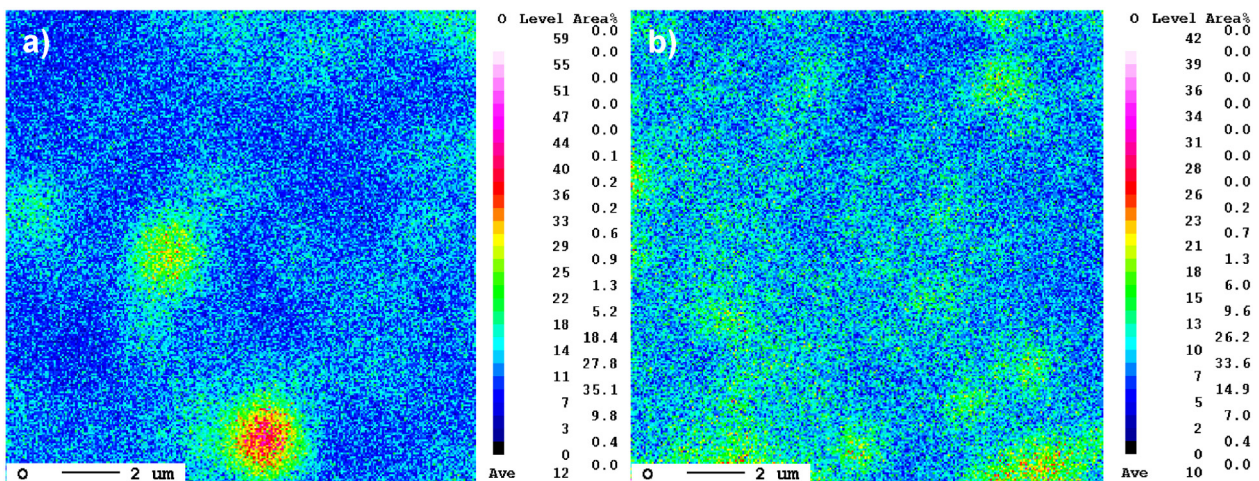


Fig. 2. The EPMA mapping of O element to represent the SiO_2 distribution on the surface of (a) Si_{PEG} and (b) fresh $\text{Si}(0)$ after the reaction with Tris buffer for 6 h at pH 8.3 ± 0.1 .

Si_{PEG} , clearly showing that SiO_2 was widely and homogeneously produced on the surface of $\text{Si}(0)$. This result clearly demonstrates that addition of PEG can not only prevent the formation of SiO_2 but also change the distribution patterns of SiO_2 from homogeneous distribution to discrete and localized dispersion, leading to the increase in reactivity of $\text{Si}(0)$.

3.2. Effect of Ni(II) concentration on the dechlorination of PCE by Si_{PEG}

The synergistic effect of Ni(II) and PEG on the dechlorination of PCE by Si_{PEG} was further examined. Fig. S5 shows the dechlorination of PCE by Si_{PEG} in the presence of various concentrations of Ni(II). The dechlorination efficiency of PCE by Si_{PEG} increased upon increasing Ni(II) concentrations from 0.02 to 0.7 mM and then decreased at a high loading of Ni(II). The dechlorination efficiency of PCE by Si_{PEG} increased from 92% at 0.02 mM Ni(II) to >98% at 0.7 mM Ni(II) in the first 4 h of incubation. However, the dechlorination efficiency decreased when the added Ni(II) concentration was higher than 1 mM and only 29% of the original PCE was dechlorinated at 2 mM Ni(II) after 4 h of incubation.

The dechlorination rate of PCE by Si_{PEG} in the presence of Ni ions followed the pseudo-first-order kinetics and the k_{obs} for PCE dechlorination is highly dependent on the mass loading of Ni(II) ranging from 0.001 to 2 mM. As shown in Fig. 3, the k_{obs} for

PCE dechlorination increased significantly from $0.36 \pm 0.02 \text{ h}^{-1}$ in the absence of Ni(II) to $0.63 \pm 0.02 \text{ h}^{-1}$ at 0.1 mM (0.3 wt%) and then leveled off to the plateau of $(0.76 \pm 0.08) \text{ to } (0.8 \pm 0.05) \text{ h}^{-1}$ when further increased the Ni(II) concentration to 0.3–0.7 mM (0.9–2.1 wt%). However, high loading of Ni(II) inhibited the dechlorination efficiency and rate of PCE by Si_{PEG} and the k_{obs} for PCE dechlorination decreased to 0.67 ± 0.02 and $0.07 \pm 0.004 \text{ h}^{-1}$ at 1.0 and 2.0 mM Ni(II), respectively.

Addition of catalytic metal ions to zerovalent metals has been reported to significantly enhance the dechlorination efficiency and rate of chlorinated hydrocarbons [11,28,29]. An optimal mass loading usually exists in a wide variety of bimetallic catalysts [30–33]. Our previous study has shown that addition of Ni(II) significantly increased the dechlorination rate of PCE by $\text{Si}(0)$ and an optimal mass loading of Ni(II) at 0.5 mM Ni(II) was obtained [11]. In this study, the maximum k_{obs} for PCE dechlorination ($0.76\text{--}0.8 \text{ h}^{-1}$) by Si_{PEG} was obtained in a wide range of 0.3–0.7 mM Ni(II), which is different from the reported results that the maximum k_{obs} only occurred at an optimal concentration. This indicates that the mechanism for PCE dechlorination by Si_{PEG} in the presence of nickel ions may be different from the reported phenomena, which states that the dechlorination rate of PCE increased at high loadings of catalytic secondary ions and then decreased dramatically after reaching the maximum rate of dechlorination [11,23,32].

3.3. Possible mechanisms for enhanced PCE dechlorination

Several mechanisms including the formation of Galvanic cell [34] and particle aggregation of second catalytic metal [11] have been proposed to explain the dechlorination of chlorinated hydrocarbons by various bimetallic materials. However, these mechanisms cannot be used to well describe the phenomenon obtained in this study that the maximum k_{obs} exists over a wide range of Ni(II) loading. The synergistic effect of Ni ions and PEG on the dechlorination of PCE by $\text{Si}(0)$ is one of the possibilities for the plateau of maximum k_{obs} . Our previous studies have indicated that the k_{obs} for PCE dechlorination by $\text{Si}(0)$ in the presence of Ni(II) and PEG was 15.3 and 106 times higher than that by $\text{Si}(0)$ alone, respectively [10,11]. In this study, the k_{obs} for PCE dechlorination by Si_{PEG} in the presence of Ni(II) increased by factors of 220–235 when compared with $\text{Si}(0)$ alone, clearly demonstrating the synergistic effect of Ni(II) and PEG on the dechlorination of PCE. Fig. 4 shows the SEM images of Si_{PEG} before and after the addition of 1 mM nickel ions and the EDS spectra of bimetallic Ni/ Si_{PEG} particles. The back scattering SEM images clearly showed that the Ni nanoparticles with

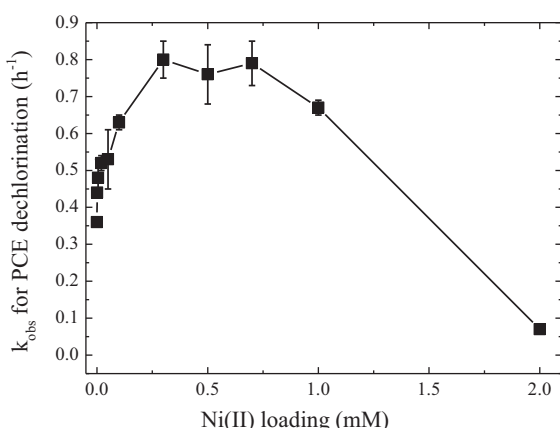


Fig. 3. The pseudo-first-order rate constant (k_{obs}) for PCE dechlorination by Si_{PEG} as a function of Ni(II) concentration ranging from 0.001 to 2 mM at pH 8.3 ± 0.1 . The error bars represent the relative standard deviation for triplicate experiments.

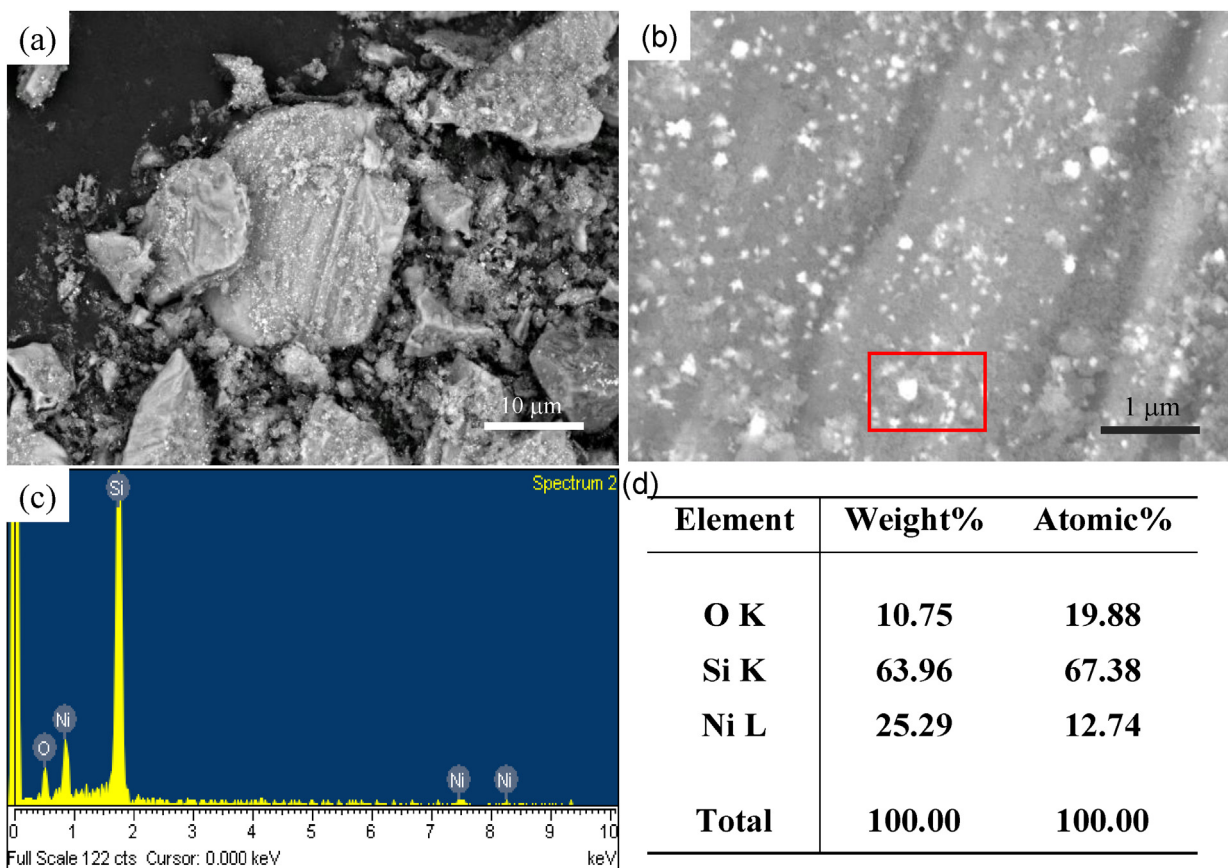


Fig. 4. The back scattering SEM imaged of bimetallic Ni/Si_{PEG} in the presence of 1 mM Ni(II). (a) and (b) are SEM images of bimetallic Ni/Si_{PEG} particles with low and high magnification, respectively. (c) is the EDS spectrum and (s) is the elemental ratio of Ni/Si_{PEG}.

average diameter of 100 nm were deposited separately onto the surface of Si_{PEG} (Fig. 4a and b). The EDS results, which obtained from the area marked in Fig. 4b, indicated that the surface of Si_{PEG} only contained silicon and nickel species, and the weight percentage of Ni on the surface was 25.3 wt% (Fig. 4c). Several studies have depicted that the high and stable dechlorination reactivity of bimetallic system is attributed to the homogeneous distribution of catalytic metal [35], which means that the increased dechlorination rate of PCE in Ni/Si_{PEG} system is not only mainly from the coated PEG on silicon surface but may also be attributed to the discrete and localized distribution of reduced nickel metal on Si_{PEG} surfaces. It should be noted that EDS is a semi-quantitative technique, and other analytical techniques such as inductively coupled plasma-mass spectroscopy and atomic absorption spectroscopy should be used when the actual concentration of Ni on Si_{PEG} is needed.

Surface coverage of Ni onto Si_{PEG} is another plausible reason for the enhanced dechlorination efficiency and rate of PCE by Si_{PEG} in the presence of Ni(II) [24,28,32,36]. Nutt et al. [32,36] used bimetallic Pd-on-Au catalysts for the dechlorination of TCE under anoxic conditions. The k_{obs} for TCE dechlorination increased as the Pd loading increased from the absent to 12.7 wt%, and then maintained at the maximum value of $31.6 \pm 0.9 \text{ L g-Pd}^{-1} \text{ h}^{-1}$ when the mass loading of Pd further increased to 17.9 wt% [32]. However, the reaction rate dropped dramatically when the Pd loading increased to 20 wt%, the calculated value needed for Pd to completely cover onto Au surface. In addition, the surface coverage has been used to explain the effect of various loadings of Cu(II) on the dechlorination of PCE and 1,1,1-trichloroethane by Si(0) and Fe(0), respectively, under anoxic conditions [24,28].

To elucidate the surface coverage of Ni onto Si_{PEG}, EPMA was further used to characterize the distribution patterns of Ni and Si

elements. Fig. 5 shows the EPMA elemental mapping images for various loadings of Ni(II) onto Si_{PEG} surface. Results clearly showed that the distribution of nickel species on the surface changed from sparse to homogeneous when the mass loading of nickel ions increased from 0.1 to 0.5 mM. However, the Ni nanoparticles aggregated into large particles at 1 mM Ni(II) and then occupied most of the active sites of Si_{PEG} at 2 mM Ni(II), resulting in the decrease in k_{obs} for PCE dechlorination. The EPMA elemental maps of Si displayed in Fig. S6 also showed the similar result that the Si element on Si_{PEG} surface was almost covered by Ni species when the loaded Ni(II) was 2 mM. These results clearly indicate that the surface coverage of Ni onto Si_{PEG} surface plays an important role in determination of dechlorination efficiency and rate of PCE by Si_{PEG} under anoxic conditions.

3.4. Product distribution

The dechlorination of chlorinated hydrocarbons by reductive metals involves hydrogenolysis and hydrodechlorination [5,29,37,38]. Previous studies have shown that PCE could be dechlorinated by Si(0) alone to produce TCE within 350 h [10,11]. However, TCE and *cis*-dichloroethylene (DCE) were found as the major products for PCE dechlorination by Si(0) when PEG was added to the Si(0) solutions [10]. In addition, the dechlorination pathway changed from hydrogenolysis to hydrodechlorination for PCE dechlorination by bimetallic Ni/Si materials and ethane was the main product, showing that the product distribution changes in the various Si-based systems [11,39].

Fig. 6 shows the product distribution of PCE dechlorination by Si_{PEG} in the presence of various concentrations of Ni(II) after 6 h of incubation. In the absence of Ni(II), TCE, *cis*-DCE, and

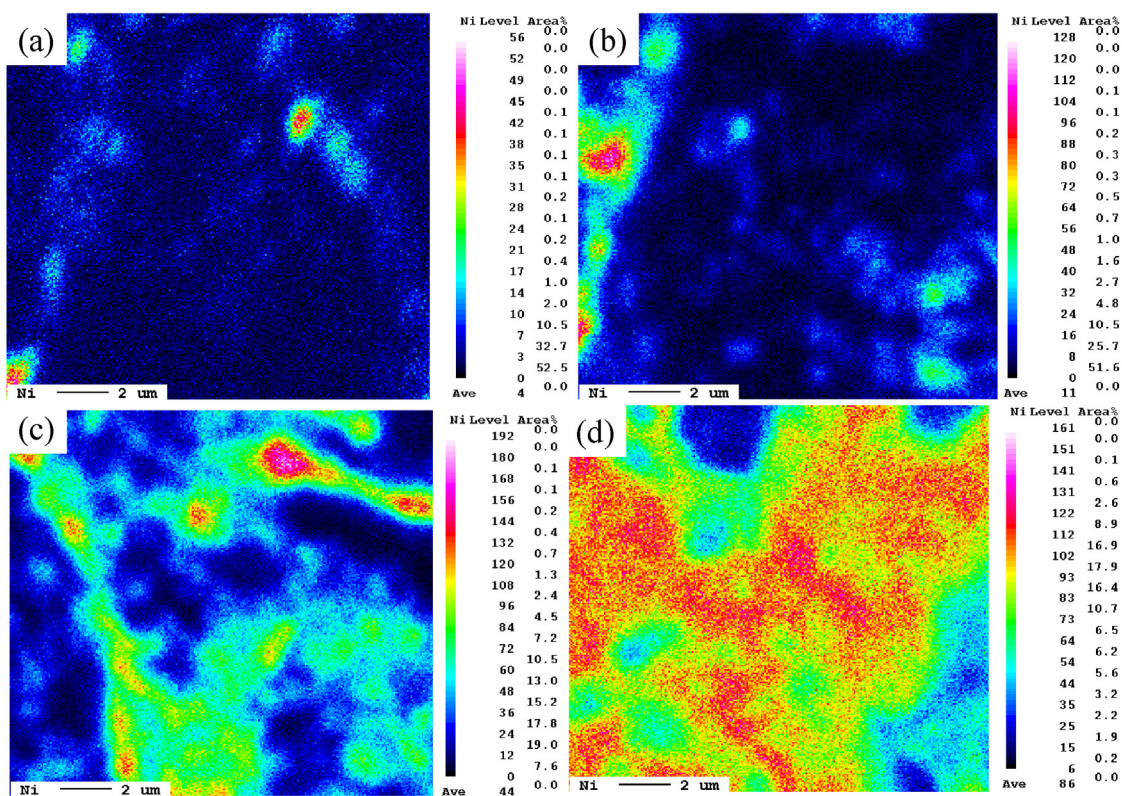


Fig. 5. The EMPA mapping of (a) 0.1 mM (0.3 wt%), (b) 0.5 mM (1.5 wt%), (c) 1 mM (3 wt%), and (d) 2 mM (6 wt%) of Ni on Si_{PEG} surface.

dichloroethyne (DCY) were detected as the major products of PCE dechlorination by Si_{PEG}, which was in good agreement with the result obtained from the previous study [10]. It is noted that PCE could undergo the reductive β -elimination, α -elimination, and hydrogenolysis, and the major products for PCE dechlorination were DCY, cis-DCE and TCE, respectively. In this study, the distribution ratios of product were 67% for TCE, 12% for cis-DCE, and 1.6% for DCY, and the concentration of acetylene and ethylene were lower than the detection limits, clearly indicating that hydrogenolysis and α -elimination were the major reaction pathways for PCE dechlorination by Si_{PEG}.

Different from the product distribution of PCE dechlorination in the absence of Ni(II), both TCE and ethane were found as the major

products for PCE dechlorination by Si_{PEG} in the presence of various loadings of Ni(II) ranging from 0.001 to 1 mM, which indicates the simultaneous occurrence of hydrogenolysis and hydrodechlorination. The formation ratios of TCE and ethane maintained at 58–62% and 15%, respectively, when the Ni(II) concentration was lower than 0.1 mM. In addition, the production ratio of ethane increased positively from 15% to 63% with the concomitant decrease in TCE ratio from 62% to 26% when the nickel loading increased from 0.001 to 0.7 mM. However, the production of ethane decreased dramatically at 1 mM Ni(II). TCE, cis-DCE, dichloroethyne, and ethane were again became the dechlorination products at 2 mM Ni(II), showing that the product distribution for PCE dechlorination by Si_{PEG} is highly dependent on the mass loading of Ni(II). It is noteworthy that TCE can be further dechlorinated to ethane by Si_{PEG}. Table S2 shows the ratio of product distribution for PCE dechlorination by Si_{PEG} in the presence of 0.1–1 mM Ni(II) after 24 h of incubation. It is clear that the ratios of TCE decreased from 26–62% at 6 h to 9–23% at 24 h, while the formation ratios of ethane increased to 76–89%. The total carbon mass balances were in the range 83–98%, clearly indicating that hydrodechlorination is a major reaction pathway for PCE dechlorination by Si_{PEG} in the presence of 0.1–1 mM Ni(II).

To further illustrate the relationship of hydrogenolysis and hydrodechlorination at various Ni(II) loadings, the pseudo-first-order formation rate constants (k_f) of ethane and TCE were calculated according to the produced concentrations of these compounds. Fig. S7 shows the k_f for ethane and TCE production from the dechlorination of PCE by Si_{PEG} in the presence of 0.001–2 mM Ni(II). The k_f for TCE formation maintained at $0.36 \pm 0.04 \text{ h}^{-1}$ when the Ni(II) concentrations were in the range 0–0.05 mM and then slightly increased to the maximum value of $0.43 \pm 0.02 \text{ h}^{-1}$ at 0.1 mM Ni(II). Further increase in Ni(II) concentration decreased the k_f for TCE formation to $0.34 \pm 0.03 \text{ h}^{-1}$ at 1 mM Ni(II) and then decreased to 0.07 h^{-1} at 2 mM Ni(II).

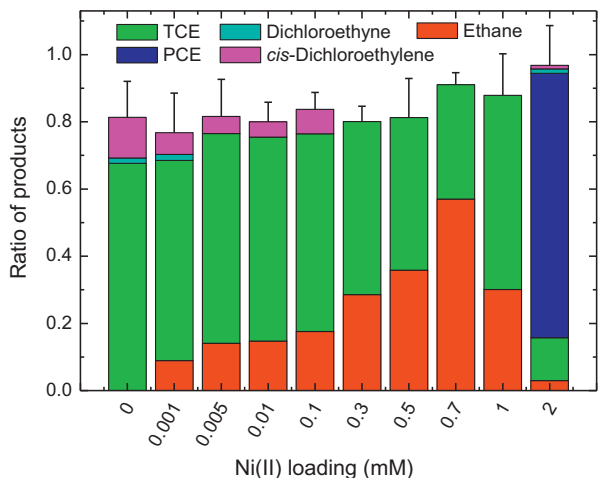


Fig. 6. Product distribution of PCE dechlorination by Si_{PEG} in the presence of various mass loading of Ni(II) ranging from 0 to 2 mM.

Different from the k_f for TCE formation, the k_f for ethane formation increased upon increasing Ni(II) concentrations at 0.001–0.1 mM and then leveled off to a plateau of $0.52 \pm 0.03 \text{ h}^{-1}$ at 0.3–1 mM. Further increasing the Ni(II) concentration to 2 mM significantly decreased the k_f for ethane formation to 0.008 h^{-1} , which is similar to the trend of k_{obs} for PCE dechlorination. This result also shows that hydrogenolysis plays an important role in PCE dechlorination by Si_{PEG} when the Ni(II) concentration was lower than 0.1 mM, while hydrodechlorination is the major reaction mechanism for PCE dechlorination at 0.3–1 mM Ni(II).

4. Conclusions

In this study, we have first demonstrated the synergistic effect of Ni(II) and PEG on the enhanced dechlorination of PCE by Si(0) under anoxic conditions. The production of metal oxides on the ZVI surface is usually a major limitation for long-term application in remediation of contaminated sites. The PEG pre-coated Si(0) has been demonstrated to be a potential material for prevention of the accumulation of oxide layers (SiO_2) on the surface, and subsequently enhances the dechlorination efficiency and rate of chlorinated hydrocarbons under anoxic conditions. Moreover, the k_{obs} for PCE dechlorination by bimetallic Ni/Si_{PEG} increased by factors of 220–235, while only 15- and 106-fold increase in k_{obs} for PCE dechlorination by Si(0) were obtained in the presence of Ni(II) and PEG, respectively, clearly showing the synergistic effect when Si_{PEG} was incorporated with nickel ions. Hydrogenolysis and hydrodechlorination occurred simultaneously for PCE dechlorination by bimetallic Ni/Si_{PEG} system in the presence of Ni(II) ions, and the product distribution was highly dependent on the mass loading of Ni ions. Hydrogenolysis played an important role in PCE dechlorination by Si_{PEG} when the Ni(II) concentration was lower than 0.1 mM, while hydrodechlorination was the major reaction mechanism for PCE dechlorination at 0.3–1 mM Ni(II). Results obtained in this study clearly indicate that only trace amount of Ni(II) is sufficient to effectively enhance the dechlorination of efficiency and rate of PCE dechlorination and change the product distribution in the presence of Si_{PEG}. This gives great impetus to coupled reduction of heavy metals and chlorinated hydrocarbons by PEG-precoated Si(0) under anoxic conditions. Ni(II) in the contaminated sites can be adsorbed by PEG and then converts to Ni(0) to form bimetallic Ni/Si_{PEG} system, resulting in the enhancement of dechlorination efficiency and rate of chlorinated hydrocarbons.

Acknowledgement

The authors thank the National Science Council, Taiwan for the financial support under contract No. NSC101-2221-E-007-084-MY3, and Ms. Y. S. Lin at National Chung Hsing University for SEM analysis.

Appendix A. Supplementary data

Supplementary data associated with this article can be found, in the online version, at <http://dx.doi.org/10.1016/j.apcatb.2013.06.033>.

References

- [1] R.A. Crane, T.B. Scott, Journal of Hazardous Materials 211 (2012) 112–125.
- [2] T. Phenrat, F. Fagerlund, T. Illangasekare, G.V. Lowry, R.D. Tilton, Environmental Science and Technology 45 (2011) 6102–6109.
- [3] G.K. Parshetti, R.A. Doong, Water Research 45 (2011) 4198–4210.
- [4] Q. Wang, S. Snyder, J. Kim, H. Choi, Environmental Science and Technology 43 (2009) 3292–3299.
- [5] S.H. Kang, W. Choi, Environmental Science and Technology 43 (2009) 878–883.
- [6] R.A. Maithreepala, R.A. Doong, Environmental Science and Technology 39 (2005) 4082–4090.
- [7] H.S. Kim, T. Kim, J.Y. Ahn, K.Y. Hwang, J.Y. Park, T.T. Lim, I. Hwang, Chemical Engineering Journal 197 (2012) 16–23.
- [8] Y.Q. Liu, S.A. Jajetich, R.D. Tilton, D.S. Sholl, G.V. Lowry, Environmental Science and Technology 39 (2005) 1338–1345.
- [9] L. Melnyk, V. Goncharuk, I. Butynk, E. Tsapiuk, Desalination 185 (2005) 147–157.
- [10] C.C. Lee, R.A. Doong, Environmental Science and Technology 45 (2011) 2301–2307.
- [11] C.C. Lee, R.A. Doong, Environmental Science and Technology 42 (2008) 4752–4757.
- [12] R.A. Doong, K.T. Chen, H.C. Tsai, Environmental Science and Technology 37 (2003) 2575–2581.
- [13] H.L. Lien, W.X. Zhang, Applied Catalysis B-Environmental 77 (2007) 110–116.
- [14] F. He, D.Y. Zhao, J.C. Liu, C.B. Roberts, Industrial and Engineering Chemistry Research 46 (2007) 29–34.
- [15] J.J. Wei, X.H. Xu, Y. Liu, D.H. Wang, Water Research 40 (2006) 348–354.
- [16] Y.H. Shih, M.Y. Chen, Y.F. Su, Applied Catalysis B-Environmental 105 (2011) 24–29.
- [17] Z.H. Zheng, S.H. Yuan, Y. Liu, X.H. Lu, J.Z. Wan, X.H. Wu, J. Chen, Journal of Hazardous Materials 170 (2009) 895–901.
- [18] B.W. Zhu, T.T. Lim, J. Feng, Environmental Science and Technology 42 (2008) 4513–4519.
- [19] S. Chatterjee, S.R. Lim, S.H. Woo, Chemical Engineering Journal 160 (2010) 27–32.
- [20] B.K. Amos, R.C. Daprato, J.B. Hughes, K.D. Pennell, F.E. Loffler, Environmental Science and Technology 41 (2007) 1710–1716.
- [21] D.S. Alessi, Z.H. Li, Environmental Science and Technology 35 (2001) 3713–3717.
- [22] G.K. Parshetti, R.A. Doong, Water Research 43 (2009) 3086–3094.
- [23] J. Xu, D. Bhattacharyya, Environmental Progress 24 (2005) 358–366.
- [24] C.C. Lee, R.A. Doong, Water Science and Technology 62 (2010) 28–35.
- [25] Z.T. Zhang, L.M. Yang, Y.J. Wang, G.S. Luo, Y.Y. Dai, Microporous and Mesoporous Materials 115 (2008) 447–453.
- [26] N. Derkaoui, S. Said, Y. Grohens, R. Olier, M. Privat, Langmuir 23 (2007) 6631–6637.
- [27] X.Y. Liu, M. Wazne, T.M. Chou, R. Xiao, S.Y. Xu, Water Research 45 (2011) 105–112.
- [28] S.J. Bransfield, D.M. Cwiertny, A.L. Roberts, D.H. Fairbrother, Environmental Science and Technology 40 (2006) 1485–1490.
- [29] T. Zhou, Y.Z. Li, T.T. Lim, Sepation Purification Technology 76 (2010) 206–214.
- [30] C. Chang, F. Lian, L.Y. Zhu, Environmental Pollution 159 (2011) 2507–2514.
- [31] N.R. Zhu, H.W. Luan, S.H. Yuan, J. Chen, X.H. Wu, L.L. Wang, Journal of Hazardous Materials 176 (2010) 1101–1105.
- [32] M.O. Nutt, J.B. Hughes, M.S. Wong, Environmental Science and Technology 39 (2005) 1346–1353.
- [33] D.M. Cwiertny, S.J. Bransfield, K.J.T. Livi, D.H. Fairbrother, A.L. Roberts, Environmental Science and Technology 40 (2006) 6837–6843.
- [34] Y.H. Liou, S.L. Lo, C.J. Lin, C.Y. Hu, W.H. Kuan, S.C. Weng, Environmental Science and Technology 39 (2005) 9643–9648.
- [35] F.Y. Xu, S.B. Deng, J. Xu, W. Zhang, M. Wu, B. Wang, J. Huang, G. Yu, Environmental Science and Technology 46 (2012) 4576–4582.
- [36] M.O. Nutt, K.N. Heck, P. Alvarez, M.S. Wong, Applied Catalysis B-Environmental 69 (2006) 115–125.
- [37] C. Amorim, M.A. Keane, Journal of Hazardous Materials 211 (2012) 208–217.
- [38] N.M. Zhu, F.S. Yi-Li, Zhang, Chemical Engineering Journal 171 (2011) 919–925.
- [39] S.J. Li, Y.L. Fang, C.D. Romanczuk, Z.H. Jin, T.L. Li, M.S. Wong, Applied Catalysis B-Environmental 125 (2012) 95–102.